Plant, Cell and Environment (2004) **27**, 1487–1502

A new analytical model for whole-leaf potential electron transport rate

T. N. BUCKLEY & G. D. FARQUHAR

Environmental Biology Group & Cooperative Research Centre for Greenhouse Accounting, Research School of Biological Sciences, The Australian National University, GPO Box 475, Canberra, ACT 2601 Australia

ABSTRACT

A new analytical model for the response of whole-leaf potential electron transport rate (*J*) to light is presented. The model treats incident irradiance at the upper and lower leaf surfaces independently, describes transdermal profiles of light absorption and electron transport capacity explicitly, and calculates *J* by integrating the minimum of light- and capacity-limited rates among paradermal chlorophyll layers. The capacity profile is assumed to be a weighted average of two opposed exponential profiles, each of which corresponds to the profile of light-limited rate when only one surface is illuminated; the weights may take on any values, provided they sum to unity, so the model can describe leaves with a wide range of 'preferred' illumination regimes. By treating irradiance at either surface independently and assuming the capacity profile is fixed on short time scales, the model predicts observed effects of leaf inversion on light-response curves and their apparent convexity. By assuming the capacity profile can adapt on developmental time scales, the model can predict the observed dependence of inversion effects on the growth lighting regime. It is suggested that the new model, which is mathematically compact and formally similar to the standard non-rectangular hyperbola model for *J*, be used in place of the standard model in studies in which the effects of leaf angle or diffuse light fraction on gas exchange are of interest.

Key-words: electron transport; gas exchange; light response; photosynthesis.

INTRODUCTION

Many gas exchange models predict net CO_2 assimilation rate using the biochemical model of Farquhar, von Caemmerer & Berry (1980), which is based on steady-state Rubisco kinetics and on the linked stoichiometries of the Calvin cycle, photosynthetic electron transport and photorespiration. In that model, the actual rate of thylakoid electron transport per unit of chlorophyll (j_a) may be limited by the sink strength of the Calvin cycle for NADPH and ATP, and hence by CO_2 availability; by the supply of energized electrons, and hence by the rate of light absorption; or by the electron transport capacity of thylakoids themselves. Various labels are used to denote electron transport rate in the limiting cases where one of more of these constraints is imagined to be negligible. For example, the 'potential electron transport rate', denoted j (or J at the leaf scale), is the actual rate in the presence of saturating $NADP^+$ and ADP.

The potential electron transport rate, like the actual rate, can also be described in terms of limiting values. In this case there are two limiting values: j_i, the rate at which electrons are supplied by photo-oxidation of water at PSII, and j_m, the electron transport capacity or 'maximum potential electron transport rate.' j_i is proportional to the rate of light absorption, so it approaches zero at low light, but may exceed j_m at high light. j can not exceed either of these limiting values, so it behaves roughly as the minimum of j_i and j_m. In practice, however, j may be lower than either j_i or j_m and is thus calculated as a *hyperbolic minimum* of j_i and j_m (Farquhar & Wong 1984): $j = \mathrm{minh}\{j_i, j_m, \theta_j\}^O\ j_i + j_m - ((j_i + j_m)^2 - 4\theta_j\ j_i j_m)^{0.5}/2\theta_j$. When the parameter θ_j equals 1, this expression degenerates to a simple minimum (i.e. $\mathrm{minh}\{j_i, j_m, 1\} = \min\{j_i, j_m\}$), but for $\theta_j < 1$, j is always less than $\min\{j_i, j_m\}$. Hence, θ_j is a measure of 'co-limitation' of electron transport by light and capacity.

A problem arises when this model is applied to whole leaves. Because light absorption and electron transport capacity generally vary among paradermal layers in intact leaves, $j = \mathrm{minh}\{j_i, j_m, \theta_j\}$does not generally imply $J = \mathrm{minh}\{J_i, J_m, \Theta_j\}$(where J_i, J_m and J are the integrals of j_i, j_m and j, respectively, over the leaf). This problem is conventionally evaded by assuming that the ratio j_m/j_i is constant among paradermal layers in a leaf at a given incident irradiance (physiologically, this means electron transport capacity is allocated in proportion to light absorption). This assumption renders the *minh* function 'scale-invariant' (Farquhar 1989), which means that the same formal relationship holds between integrals of the independent variables over any scale. Hence, whole-leaf potential electron transport rate, J, is conventionally modelled as

Correspondence: Thomas N. Buckley. Fax: +61 2 6125-4919; e-mail: tom_buckley@alumni.jmu.edu

$$J = \frac{J_i + J_m - \sqrt{(J_i + J_m)^2 - 4\Theta_J J_i J_m}}{2\Theta_J} = \min\{J_i, J_m, \Theta_J\}, \quad (1)$$

Equation 1 (Fig. 1) is used in most models of leaf and canopy gas exchange. Typically, J_i is assumed proportional to incident irradiance, J_m is either estimated from the value of J at saturating light or assumed proportional to carboxylation capacity, and Θ_J is either fitted to light-response curves or treated as a constant and taken from the literature.

The assumption underlying Eqn 1 – that j_m is proportional to j_i among paradermal layers – would appear to be supported by the observed similarity between transdermal profiles of photosynthetic capacity and light absorption under controlled conditions (Evans 1995; Evans & Vogelmann 2003). However, the transdermal light profile is controlled by the irradiances at both the upper and lower leaf surfaces, and these irradiances can vary independently as leaves flutter in the wind, as the sun moves through the sky, and as atmospheric conditions fluctuate, varying the proportions of collimated and isotropic (direct and diffuse) light. As a result, the transdermal profile of light absorption can also change very quickly, and probably too quickly for the capacity profile to adapt. This causes the light and capacity profiles to differ, violating the assumption of scale-invariance and rendering J sensitive to changes in the fraction of light incident on the upper surface.

Experiments have in fact shown that J is sensitive to the direction of incident light. In horizontally grown leaves, J is higher at a given irradiance when the upper surface alone is illuminated (Moss 1964; Leverenz 1988; DeLucia *et al.* 1991; Evans, Jakobsen & Ögren 1993). This can be explained by the presence of a fixed capacity profile that is biased in favour of the upper surface: when light arrives at the lower surface, light absorption is high in layers with low capacity, and low in layers with high capacity. Similarly, in vertically grown leaves, J is maximal when a given irradiance is evenly divided between the two surfaces (Evans *et al.* 1993). Furthermore, these acclimations to growth lighting regime can be overcome by applying a new lighting regime, which causes re-acclimation on time scales of several days to weeks. For instance, if a horizontally grown leaf is inverted, and then kept in that position indefinitely, it eventually 'prefers' light from what was formerly the lower surface (Ögren & Evans 1993).

These results all suggest that leaves can adapt their transdermal capacity profiles to the prevailing illumination regime on long time scales, but that on short time scales of a day or less, the capacity profile is fixed. Hence, the scale invariance assumption, and consequently Eqn 1, fails when the illumination regime differs from that to which the capacity profile is adapted. A more flexible model is required to predict the light response of potential electron transport rate and gas exchange to naturally varying light conditions.

In this study, we present a model that predicts the response of J to variable illumination of each leaf surface. The model is based on explicit transdermal profiles of light absorption and electron transport capacity, it can accommodate capacity profiles that are adapted to a range of

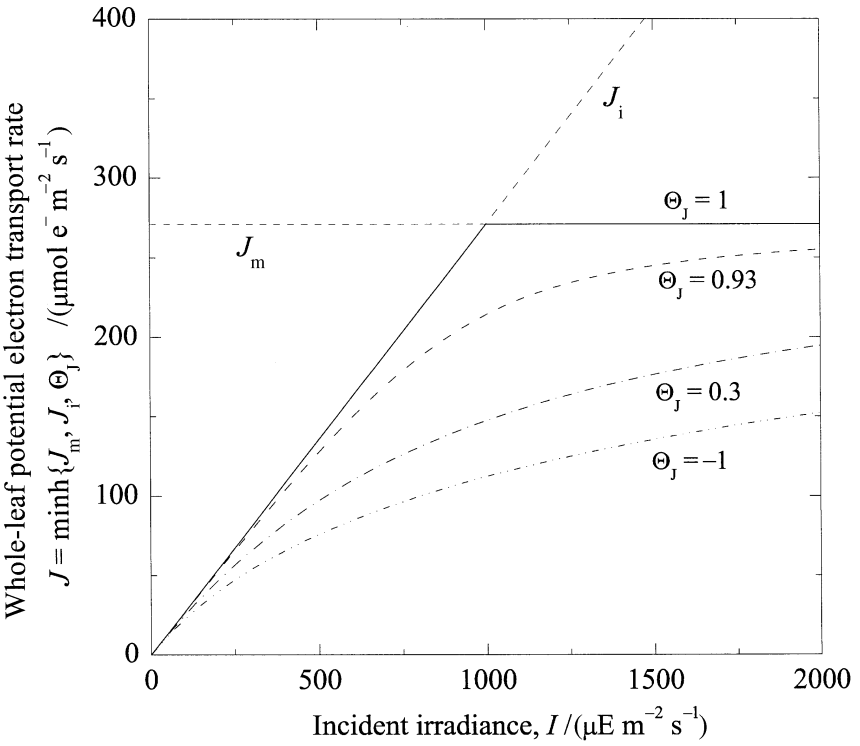

Figure 1. Diagram of the standard model for the response of whole-leaf potential electron transport rate, J, to incident irradiance, I, for different values of the convexity parameter, Θ_J. When $\Theta_J = 1$ (solid line), J is simply the minimum of the light-limited and capacity-limited potential rates (J_i and J_m, respectively; straight dashed lines). For $\Theta_J < 1$, J is always smaller than either J_i or J_m, reflecting some degree of co-limitation between light and capacity.

illumination regimes, and it is simple enough to incorporate into existing models of leaf and canopy gas exchange without great difficulty.

THE MODEL

This section presents a few key equations chosen from the detailed derivation of our model, which is given in the Appendix. We imagine the leaf to consist of many infinitesimally thin paradermal layers, each with a fixed amount of chlorophyll per unit leaf area, dc (Table 1 gives a list of symbols with descriptions and units). This defines a transdermal axis of cumulative chlorophyll content, c, ranging from 0 at the upper surface to C, the whole-leaf chlorophyll content, at the lower surface. We show in the Appendix that the transdermal profile of the rate of light absorption, $i_a(c)$, can be approximated by

$$i_a(I_u, I_l, c) = p(1-\rho)k_c'(I_u e^{-k_c c} + \tau I_l e^{k_c c}), \quad (2)$$

where I_u and I_l are the incident irradiances at the upper and lower surfaces, respectively; $p > 1$ is a factor that accounts for back-scattered light flux through the uppermost layer, which increases the space irradiance in upper layers; ρ is surface reflectance; k_c' is the absorption coefficient for white light; k_c is the sum of absorption and scattering coefficients; and $\tau = {}^{O}\exp(-k_c C)$ is leaf transmittance to non-reflected light, or $1 - \alpha/(1-\rho)$, where α is absorptance. Equation 2 is Eqn 16 in the Appendix.

The rate at which photo-oxidation of water yields energized electrons, or equivalently, the light-limited potential electron transport rate, j_i, is proportional to the rate of photon absorption by the maximum quantum yield of electrons, ϕ_m, and by a factor $1 - f'$ that accounts for the intrinsic inefficiency of photon utilization (i.e. f' is the limiting

Table 1. Terms in the model and its derivation

Description	Symbol	Units
Whole-leaf terms		
Potential electron transport rate	J	μmol e$^-$ m^{-2} s^{-1}
Light-limited potential electron transport rate	J_i	μmol e$^-$ m^{-2} s^{-1}
Maximum (capacity-limited) potential electron transport rate	J_m	μmol e$^-$ m^{-2} s^{-1}
Excess J_i in light-saturated layers when others are light-limited	J_s	μmol e$^-$ m^{-2} s^{-1}
Total incident irradiance	I	μmol e$^-$ m^{-2} s^{-1}
Incident irradiance on upper surface	I_u	μmol hν m^{-2} s^{-1}
Incident irradiance on lower surface	I_l	μmol hν m^{-2} s^{-1}
Incident irradiance at which $J_i = J_m$	$I*$	μmol hν m^{-2} s^{-1}
Convexity parameter for the standard model	Θ_J	unitless
Convexity parameter for our model	Θ_s	unitless
Value of Θ_J such that Eqns 1 and 11 match at $I = I*$	Θ_J*	unitless
Term in expression for Θ_J* that accounts for W_u, w_u and τ	z	unitless
Maximum quantum yield	ϕ_m	e$^-$/hν
Whole-leaf maximum quantum yield to incident irradiance	ϕ	e$^-$/hν
Leaf transmittance to non-reflected light	τ	unitless
Relative degree of saturation at upper (lower) surface	s_u (s_l)	unitless
Leaf absorptance	α	unitless
Leaf reflectance	ρ	unitless
Adaptive weighting of capacity profile to upper (lower) surface	w_u (w_l)	unitless
Weighting of lighting regime to upper (lower) surface, I_u/I (I_l/I)	W_u	unitless
Ratio of I_u (I_l) to $I*$	ω_u (ω_l)	unitless
Whole-leaf chlorophyll content	C	mmol Chl m^{-2}
Chlorophyll layer terms		
Cumulative chlorophyll content	c	mmol Chl m^{-2}
Chlorophyll content of infinitesimal paradermal layer	dc	mmol Chl m^{-2}
Cumulative chlorophyll content at which $j_i = j_m$	$c*$	mmol Chl m^{-2}
Sum of absorption and scattering coefficients	k_c	[mmol Chl m^{-2}]$^{-1}$
Absorption coefficient	k_c'	[mmol Chl m^{-2}]$^{-1}$
Potential electron transport rate	j	μmol e$^-$ s^{-1} mmol^{-1} Chl
Light-limited potential electron transport rate	j_i	μmol e$^-$ s^{-1} mmol^{-1} Chl
Maximum (capacity-limited) potential electron transport rate	j_m	μmol e$^-$ s^{-1} mmol^{-1} Chl
Total rate of photon absorption	i_a	μmol hν s^{-1} mmol^{-1} Chl
Photon absorption due to irradiance at upper (lower) surface	i_{au} (i_{al})	μmol hν s^{-1} mmol^{-1} Chl
Convexity parameter	θ_j	unitless
Increase in space irradiance due to intraleaf reflection	p	unitless
Fraction of absorbed photons that do not drive electron generation	f'	unitless
Pooled parameter, $\phi_m(1-f')p(1-\rho)k_c'/k_c$	F	e$^-$/hν

value, at low light, of the fraction of photons that are absorbed but do not lead to photo-oxidation of water):

$$j_i(I_u, I_l, c) = \phi_m(1-f')i_a(I_u, I_l, c) = k_c F(I_u e^{-k_c c} + \tau I_l e^{k_c c}) \quad (3)$$

where $F^\circ \equiv \phi_m(1-f')p(1-\rho)k_c'/k_c$. (Eqn 3 is Eqn 17 in the Appendix). When the rate of light absorption in a given layer is large enough to saturate downstream components of the thylakoid electron transport chain, the potential electron transport rate per unit Chl, $j(c)$, approaches the electron transport capacity, $j_m(c)$. In other words, j behaves roughly as the minimum of j_i and j_m. However, in practice, biochemical or biophysical feedbacks may cause j to be lower than either j_i or j_m, so j is modelled as a hyperbolic minimum of j_i and j_m:

$$j(I_u, I_l, c) = \text{minh}\{j_i(I_u, I_l, c), j_m(c), \theta_j\} = \frac{j_i + j_m - \sqrt{(j_i + j_m)^2 - 4\theta_j j_i j_m}}{2\theta_j} \quad (4)$$

For $\theta_j < 1$, this expression is always smaller than the simple minimum of j_i and j_m. In the special case where $\theta_j = 0$, Eqn 4 is a rectangular hyperbola, or equivalently, the harmonic sum of j_i and j_m: $j = j_i j_m/(j_i + j_m)$.

The standard model for whole-leaf potential electron transport rate, J (Eqn 1), assumes that the functional form of Eqn 4 also applies at the leaf scale, which requires in turn the assumption that j_m is proportional to j_i by the same factor in all paradermal layers. That assumption is unrealistic in situations where the ratio between I_u and I_l varies on time scales shorter than the time constant for adaptive adjustment of j_m (on the order of days to weeks; Ögren & Evans 1993). We propose a different assumption, namely that the transdermal profile of electron transport capacity reflects a compromise between perfect adaptation to illumination at the upper and lower surfaces. Formally, we hypothesize that $j_m(c)$ is a weighted average of two j_i profiles, each of which results when a single leaf surface is illuminated at some 'preferred' irradiance, I_*. The weightings for the upper and lower surfaces are denoted w_u and w_l, respectively, and they sum to unity ($w_u + w_l^\circ \equiv 1$), so the hypothesized j_m distribution is

$$j_m(c) = w_u j_i(I_*, 0, c) + w_l j_i(0, I_*, c) = k_c F I_* (w_u e^{-k_c c} + w_l \tau e^{k_c c}). \quad (5)$$

(Eqn 18 in the Appendix). For example, a leaf that is equally well adapted to illumination from either surface would have a symmetrical capacity profile, with $w_u = w_l = 0.5$: $j_m = \frac{1}{2} k_c F I_* (e^{-k_c c} + \tau e^{k_c c})$; and the profile for a leaf adapted to illumination only at the upper surface would be a simple exponential function, highest at the upper surface, that is, $w_u = 1$ and $w_l = 0$: $j_m = k_c F I_* e^{-k_c c}$. Because the light absorption profile may fluctuate diurnally, the capacity profiles created by this compromise rarely match the light profile exactly, so light and capacity are spatially decoupled under most conditions (e.g. Fig. 2c & d).

Integrating to the leaf scale

When the hyperbolic minimum model for j (Eqn 4) is applied to the expressions for j_i and j_m (Eqns 3 and 5, respectively), the resulting expression for j can not be integrated analytically to the whole leaf (see Appendix). After investigating many options for dealing with this problem, we concluded that the best approach was to assume, initially, that $\theta_j = 1$ (i.e. $j = \min\{j_i, j_m\}$), then to integrate the model to the whole leaf (Eqn 6 below), and finally to modify the integrated model to account for $\theta_j < 1$ (Eqn 11 below). This artifice yields a whole-leaf model that does not represent Eqns 3 and 5 perfectly, but is tractable and empirically adequate. The simple minimum of j_i and j_m (given by Eqns 3 and 5) can be integrated over c (as shown in the Appendix) to yield whole-leaf expressions:

$$\int_0^C \min\{j_i(c), j_m(c)\}dc = \min\{J_i - J_s, J_m\}, \quad \text{where} \quad (6)$$

$$J_i = \phi I = \phi I_u + \phi I_l \quad (7)$$

$$J_m = \phi I_* \quad (8)$$

where $I \equiv I_u + I_l$, ϕ is the initial slope of the light-response curve for J (or, in terms of the reduced quantities in our model, $\phi^O(1-\tau)F = (1-\tau)\phi_m(1-f')p(1-\rho)k_c'/k_c$). I_* is now more readily interpreted: it is the value of I at which $J_i = J_m$ (e.g. in Fig. 1, $I_* = 1000\ \mu\text{E m}^{-2}\ \text{s}^{-1}$).

The remaining term in Eqn 6, J_s, is the product of ϕ and the amount of excess light absorbed by light-saturated layers when some other layers are light-limited. This critical element of our model is discussed in detail in the next subsection. J_s is calculated by Eqns 9 and 10:

$$J_s = \frac{1}{1-\tau} \cdot \begin{cases} (\phi I_u - w_u J_m)(1-\sqrt{\tau/s_u})^2 & (a) \\ (\phi I_l - w_l J_m)(1-\sqrt{\tau/s_l})^2 & (b) \\ 0 & (c) \end{cases}$$

$$(a) \quad \text{if} \quad \tau < s_u < \tau^{-1} \quad \text{and} \quad I_u > w_u I_*$$
$$(b) \quad \text{if} \quad \tau < s_u < \tau^{-1} \quad \text{and} \quad I_l > w_l I_*$$
$$(c) \quad \text{else} \quad (9)$$

$$s_u \equiv \frac{I_u - w_u I_*}{I_l - w_l I_*} \quad \text{and} \quad s_l \equiv 1/s_u \quad (10)$$

(Note the minus sign in Eqn 10). Finally, the integral of $\min\{j_i, j_m\}$ (Eqn 6) overestimates the integral of $\text{minh}\{j_i, j_m, \theta_j\}$ if $\theta_j < 1$. One way to correct for this is to modify Eqn 6 as follows:

$$J = \text{minh}\{J_i - J_s, J_m + J_s, \Theta_s\} = \frac{J_i + J_m - \sqrt{(J_i + J_m)^2 - 4\Theta_s(J_i - J_s)(J_m + J_s)}}{2\Theta_s} \quad (11)$$

Equations 7–11 comprise our model. (Eqns 6–11 are Eqns 40, 21, 22, 39, 25 and 41), respectively, in the Appendix.)

What is J_s?

Our model is similar in form to the standard model (cf. Eqns 1 and 11), except that ours contains a new term, J_s, defined

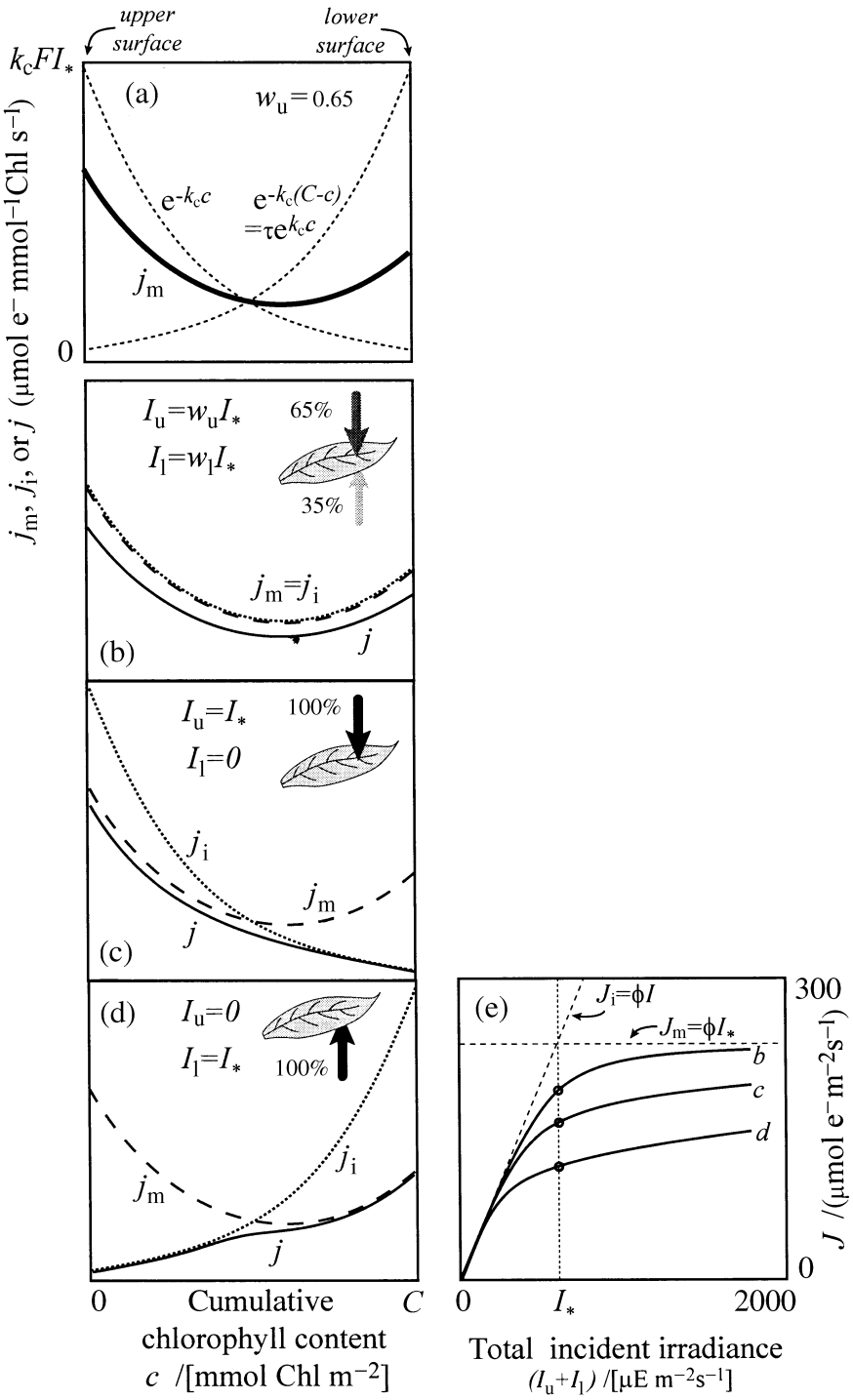

Figure 2. (a) A hypothetical transdermal profile of electron transport capacity, j_m (thick line), equal to a weighted sum of two exponential profiles (dashed lines), each of which matches the absorption profile for illumination at either surface. (b–d) Three profiles of light-limited potential electron transport rate, j_i (dotted lines), overlaid on the j_m profile (dashed lines) from (a) and showing the resultant profile of potential electron rate, j (solid lines) for $\theta_j = 0.93$. In (b), the illumination regime is optimal (65% to the upper surface, because $w_u = 0.65$), whereas in (c) and (d) only one surface (upper or lower, respectively) is lit. (e) Whole-leaf light-response curves for the leaf shown in (a), but using the lighting proportions from (b–d). J_i and J_m, the integrals of the j_i and j_m profiles shown in (a–d), are shown with dashed lines in (e).

by Eqn 9. The meaning of J_s can be understood from various perspectives. First, J_s is only non-zero when the transdermal profiles of light absorption and electron transport capacity cross one another within the leaf (e.g. Figs 2c & d, 3, 4c & d, & 5a). When the profiles do cross over, portions of them 'overlap' (e.g. shaded region in Fig. 3f). Graphically, J_s is the portion of the area under the light absorption profile ($j_i(c)$) that does not overlap the capacity profile ($j_m(c)$) (Fig. 3d). Mathematically, J_s is the integral of the difference between j_i and j_m in layers that are light saturated, when some other layers are also light-limited. More intuitively, J_s is a measure of the inefficiency caused by the mismatch between the light and capacity profiles.

Another way to interpret the integrated model is in terms of the layer-wise minima and maxima of the transdermal profiles of light absorption rate and electron transport capacity. Equation 11 calculates the hyperbolic minimum of two quantities: $J_i - J_s$ and $J_m + J_s$. The smaller of these two

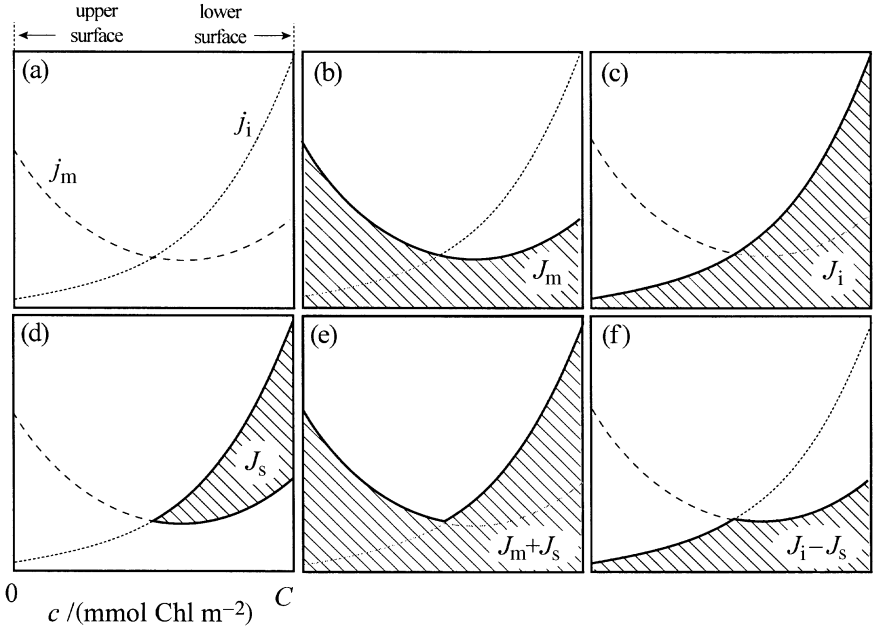

Figure 3. Geometric interpretation of integrated terms in the model. (a) Hypothetical transdermal profiles of j_m and j_i (capacity- and light-limited potential electron transport rates), taken from Fig. 2d (the upper surface is at the left side of each panel; $w_u = 0.65$, $I_u = 0$ and $I_l = I*$). (b) J_m, and (c) J_i are simply the areas under the j_m and j_i profiles, respectively. (d) J_s is the portion of the area under the j_i profile that does not overlap the j_m profile. (e) $J_m + J_s$ and (f) $J_i - J_s$ are the areas under the layerwise maxima and minima, respectively, of j_m and j_i. Our model incorporates layerwise convexity by taking the hyperbolic minimum of (e) and (f).

quantities is simply the integral of the layer-wise minima of j_i and j_m ($\int\min\{j_i, j_m\}dc$), given by Eqn 6, whereas the larger of these two quantities is the integral of the layerwise maxima of j_i and j_m ($\int\max\{j_i, j_m\}dc$). The layerwise maxima and minima are shown graphically in Fig. 3e and f, respectively. (Note that, despite the minus sign, $J_i - J_s$ is not necessarily the smaller of $J_i - J_s$ and $J_m + J_s$; for example, when $J_s = 0$ and $J_i > J_m$, as in Fig. 4b).

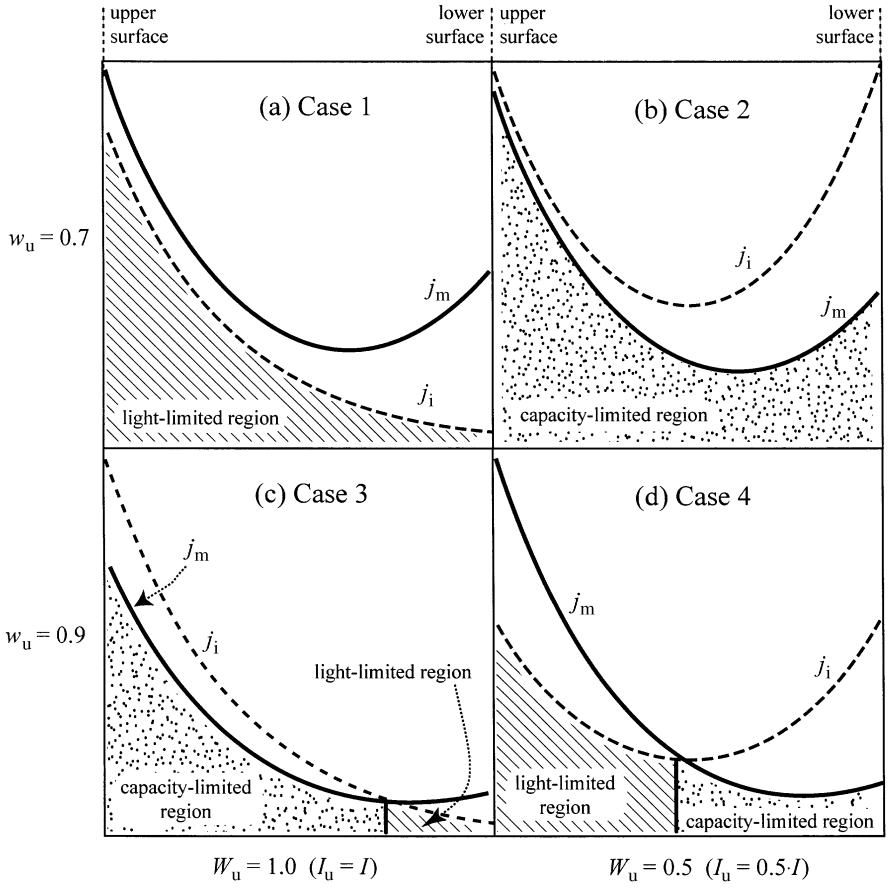

Figure 4. Illustration of four different cases for the integral of the layer-wise minimum of transdermal profiles of light absorption ($j_i(c)$) and electron transport capacity ($j_m(c)$). (a) Case 1: all layers are light-limited, so the minimum is j_i everywhere. (b) Case 2: all layers are light-saturated, so the minimum is j_m for all layers. (c),(d) Cases 3 and 4: the profiles cross over somewhere within the leaf, creating distinct light-limited and light-saturated regions that must be integrated separately. In case 3 (c), the upper surface is light-saturated, whereas in case 4 (d), the lower surface is light-saturated. [Values of w_u and W_u used to create these sample profiles are shown on the figure; the total irradiance, I, was $0.6I*$ for (a), $1.2I*$ for (b), and $1.0\ I*$ for both (c) and (d)].

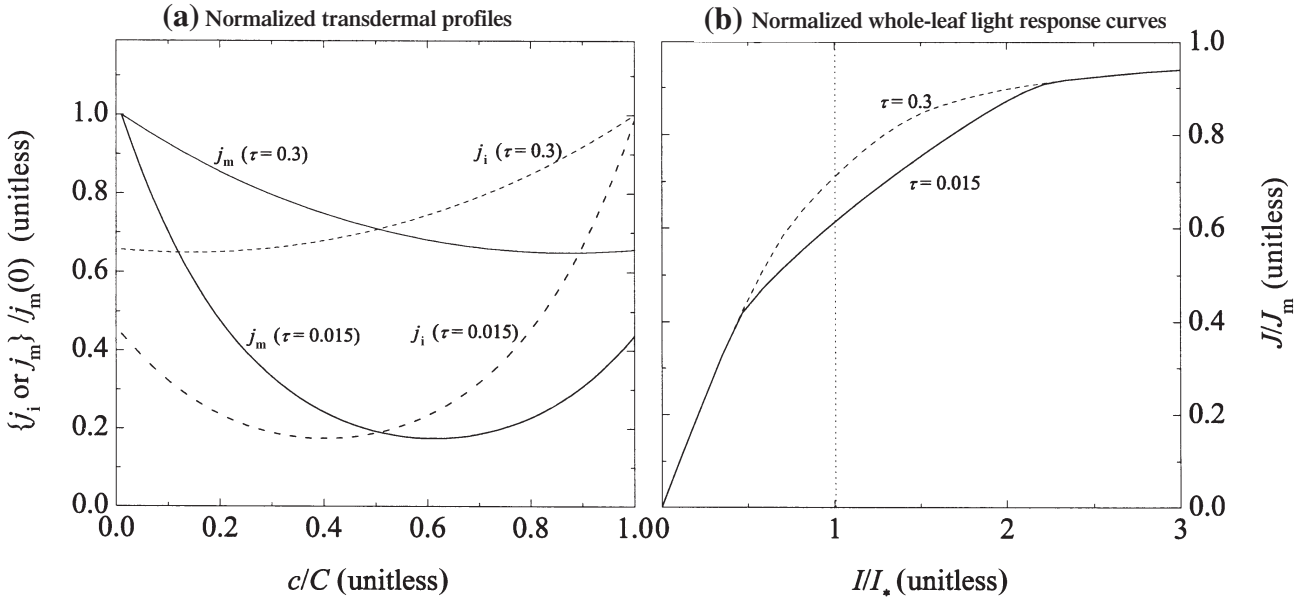

Figure 5. Comparison between two leaves whose capacity profiles have the same adaptive weighting ($w_u = 0.7$), whose upper and lower surfaces are illuminated in the same proportion ($W_u = 0.3$), and for which $I = I*$, but which have different values of τ ($\tau = 0.3$ and $\tau = 0.015$). (a) Transdermal profiles of electron transport capacity (j_m) and light-limited potential electron transport rate (j_i), expressed relative to the value of j_m at the upper surface, and plotted against the ratio of cumulative chlorophyll content (c) to whole-leaf Chl content (C). (b) Whole-leaf light-response curves for potential electron transport rate for the leaves depicted in (a), with J expressed relative to whole-leaf capacity, J_m, and total incident irradiance, I, expressed relative to $I*$ ($\Theta_s = 0.86$ for both curves). The leaf with lower transmittance captures a greater fraction of incident light than the other leaf, but has a greater relative deficit in potential electron transport rate (i.e. J/J_m is lower) when the illumination regime does not match the capacity profile.

Parameters

Our model contains seven degrees of freedom (J_m, I_u, I_l, ϕ, τ, w_u, Θ_s) – three more than the standard model's four (J_m, I, ϕ, Θ_J). One of the new degrees of freedom comes from separating irradiance into I_u and I_l, but this is properly considered an additional independent variable, rather than a parameter. The other two new degrees of freedom are required to capture salient aspects of the hypothesized transdermal capacity profiles. w_u describes the extent to which the capacity profile is skewed towards either surface. τ measures light attenuation; however, this could be described without reference to the capacity profile, and in fact τ also appears in the standard model, embedded in ϕ. The reason τ must be considered independently of ϕ in our model is that τ describes the 'depth', and thus the degree of curvature, in the exponential-based profiles of light absorption and capacity; that curvature, in turn, affects the magnitude of the deficit in whole-leaf J caused by mismatch between the two profiles. This is illustrated in Fig. 5. These curvature effects are not explicit in the standard model, so τ can, in principle, remain embedded in ϕ in that model.

The value of ϕ can be estimated for both models from the initial slope of J versus I (total incident irradiance). In the standard model, J_m and Θ_J can then be estimated by fitting Eqn 1 to J versus ϕI. In our model, J_m, Θ_s, τ and w_u can be estimated by fitting Eqn 11 to two light-response curves simultaneously, each obtained with a different measurement lighting regime. It may also be possible to estimate w_u by varying the proportions of light supplied to either surface while keeping the total constant, because the ratio of I_u to I that maximizes J should equal w_u. However, we did not attempt to test that approach.

RESULTS AND DISCUSSION

The general behaviour of our model is illustrated in Fig. 6, which shows light-response curves for leaves with different degrees of preference for illumination at the upper surface (i.e., different values for the adaptive weighting parameter, w_u), varying proportions of total irradiance supplied to the upper surface ($W_u{}^O I_u/I$), and two different values for the convexity parameter, Θ_s. Three major features of these response curves stand out. First, the value of J predicted for any given total irradiance (I) is greatest when the fraction of I supplied to the upper surface equals the adaptive weighting of the capacity profile towards that surface (that is, when $W_u = w_u$; solid lines in Fig. 6). This is because, in such cases, the ratio between light absorption rate and electron transport capacity is the same in all paradermal layers (e.g. Fig. 2c), so that neither light nor capacity is more limiting in one layer than in another. When any fraction of I other than W_u is supplied to the upper surface, however, J may be lower than for $W_u = w_u$, because in that case some layers may be light saturated at the same time that other layers are light-limited (e.g. Fig. 2d).

Second, the magnitude of the effects of lighting regime

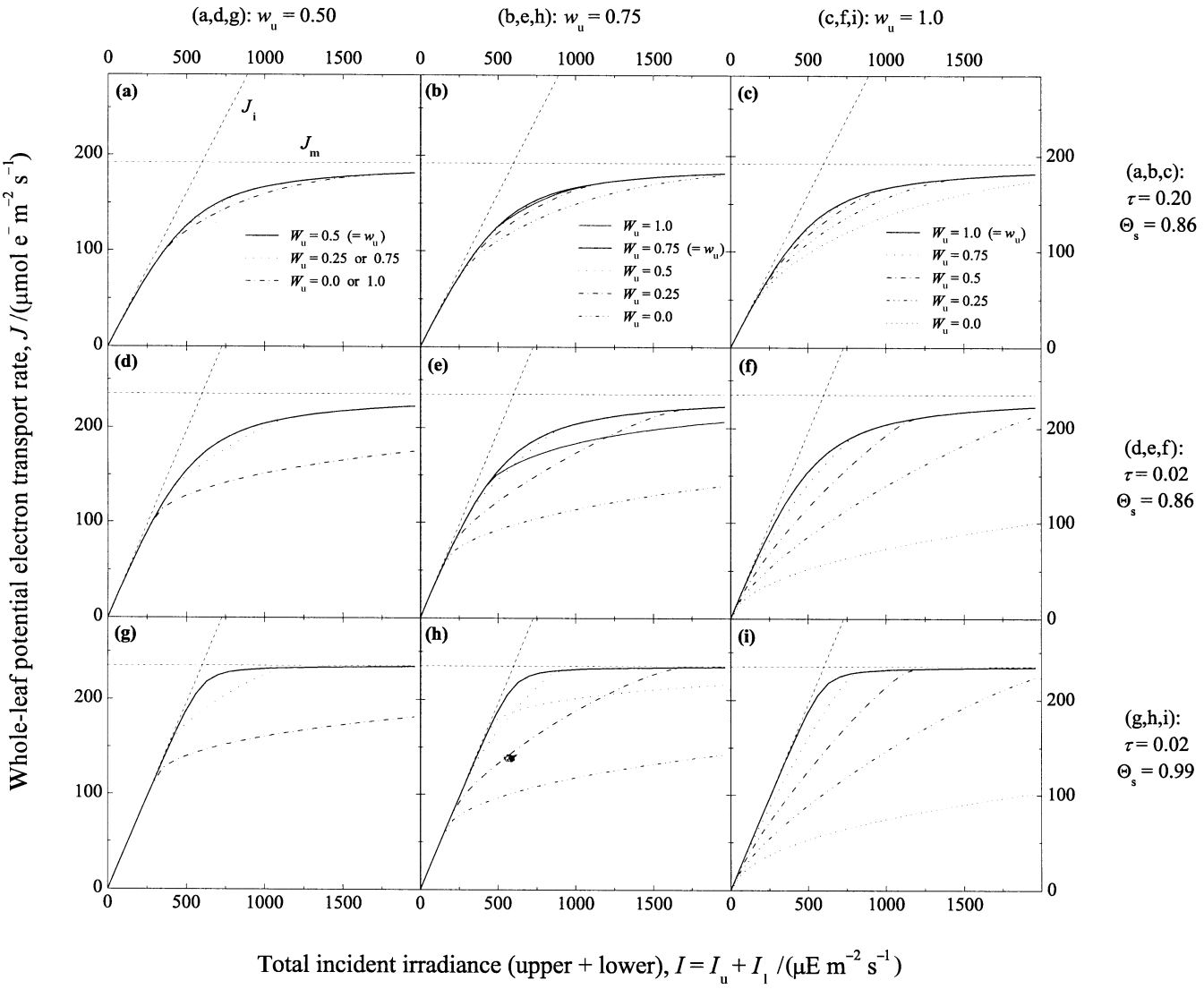

Figure 6. Light-response curves (J versus I) predicted by the model for different values of τ, w_u, I_u/I and Θ_s. (a),(b),(c): $\tau = 0.2$, $\Theta_s = 0.86$. (d),(e),(f): $\tau = 0.02$, $\Theta_s = 0.86$. (g),(h),(i): $\tau = 0.02$, $\Theta_s = 0.99$. (a),(d),(g): $w_u = 0.5$ (a perfectly isobilateral leaf). (b),(e),(h): $w_u = 0.75$ (a leaf with transdermal capacity gradient partially biased towards the upper surface). (c),(f),(i): $w_u = 1.0$ (a perfectly bifacial leaf). Within each plot, each different line represents the response curve for a different proportion of light supplied to the upper surface ($W_u = I_u/I$), as indicated by the inset legends in a-c; where line styles indicated in the legends are not visible in a plot, it is because they overlap with other lines. J_m and J_i are shown by dashed lines, as labelled in (a).

depends on the 'steepness' or curvature of the transdermal profiles of light absorption and electron transport capacity. The profiles are steeper when the total chlorophyll content (C) is high, and thus when the transmittance to non-reflected light (τ) is low (e.g. Fig. 5a); hence the difference between the light-response curves for optimal and suboptimal lighting regimes is larger in leaves with low τ (cf. the two curves in Fig. 5b and Fig. 6a–c versus 6d–f). The effects of lighting regime may be experimentally negligible in some cases (e.g. for $\tau = 0.2$ and $w_u = 0.5$, Fig. 6a), but very large in other cases (e.g. for $\tau = 0.02$ and $w_u = 1.0$, Fig. 6f). Third, in leaves whose capacity profiles are partially but not totally biased toward the upper surface (e.g. $w_u = 0.75$, Fig. 6b, e & h), illumination of the upper surface alone yields equal or greater J than illumination of the lower surface alone (cf. curves for $W_u = 1.0$ and $W_u = 0$).

These predictions are consistent with observed effects of leaf inversion and growth lighting regime on light-response curves. Evans *et al.* (1993) performed a comprehensive study of these effects for four species. They constrained growing leaves to horizontal or vertical positions to induce adaptation to illumination from one surface or both surfaces, respectively, measured light-response curves for these leaves while supplying light to one or both surfaces, and fitted the standard J model (Eqn 1) to the measured response curves. For horizontally restrained leaves, the fitted convexity parameter Θ_J was substantially higher (and thus J was higher at all irradiances) when the upper surface

was illuminated than when the lower surface was illuminated, but in vertically restrained leaves Θ_J was independent of which surface was illuminated. DeLucia *et al.* (1991) also reported that vertical leaves responded identically to light supplied at either surface, whereas horizontal leaves responded more strongly to light at the upper surface.

To demonstrate the performance of our model more directly, we fitted it to 12 of the light-response curves measured by Evans *et al.* (1993), corresponding to three lighting regimes (upper, lower, or both surfaces illuminated) for each of four plant treatments (horizontally and vertically restrained leaves in each of two species: *Eucalyptus maculata* and *E. pauciflora*) (fitting procedures are described in the Appendix). Figure 7 shows the data and the fitted model curves; each set of three modelled curves shown for each plant treatment corresponds to a single set of parameters (J_m, Θ_s, ϕ, w_u and τ). Fitted parameter values are given in Table 2. The model was able to be fitted to the data reasonably well ($r^2 > 0.99$ in all cases).

There are two immediate and testable corollaries to the hypothesis that the transdermal capacity profile adapts itself to the absorption profile. First, the responses to illu-

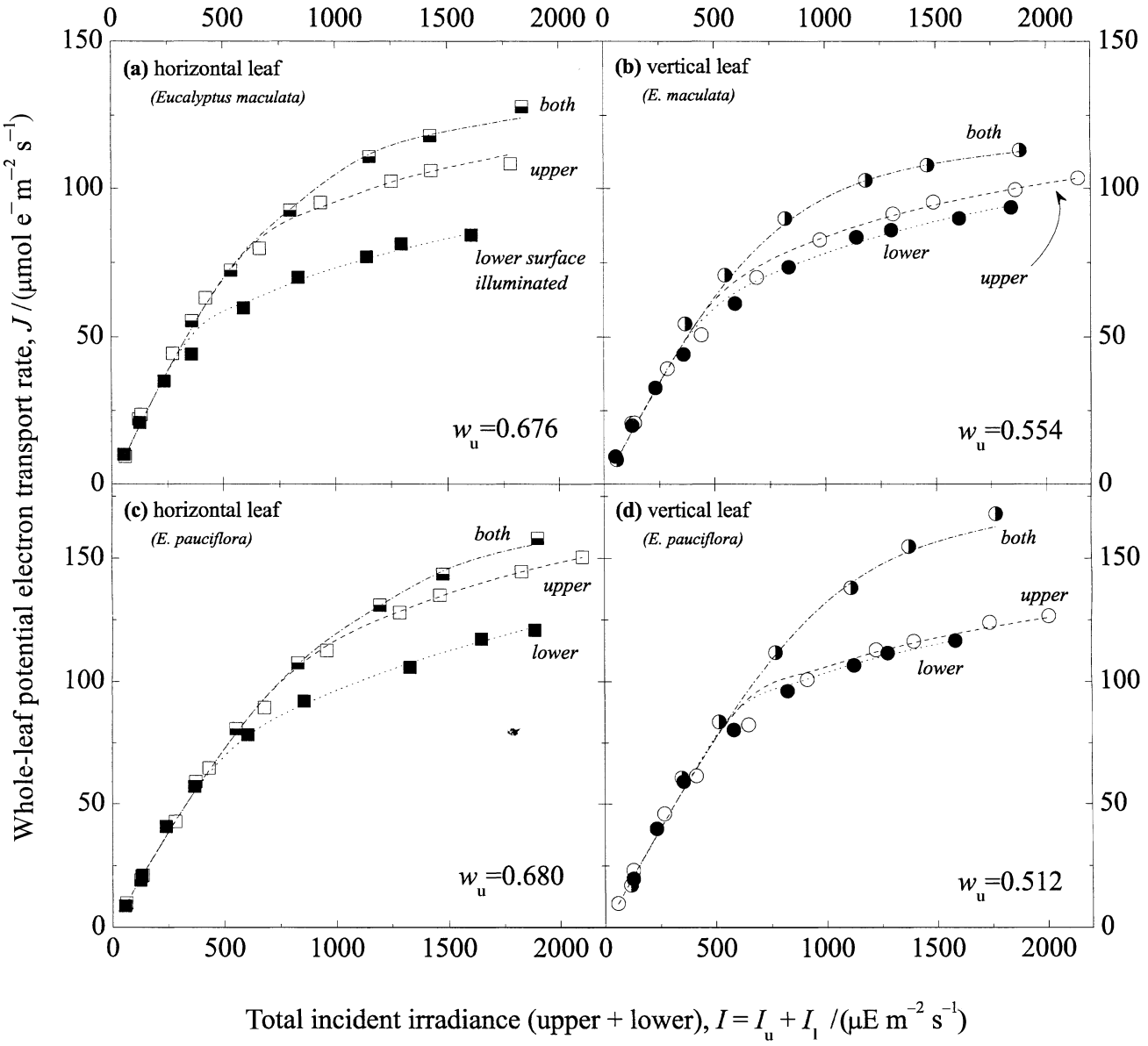

Figure 7. Symbols: observed responses of whole-leaf potential electron transport rate, J, for leaves of *Eucalyptus maculata* (a,b) and *E. pauciflora* (c,d) that were horizontally restrained (squares) or vertically restrained (circles) during development; data are shown for illumination at the upper surface (□, ○), lower surface (■, ●) or both surfaces (◒, ◑) (data from Evans *et al.* 1993). Lines: our model fitted to these data, using $W_u = 1.0$, 0.0, and 0.5 to simulate illumination at the upper, lower, and both surfaces, respectively. Fitted values of w_u, the adaptive weighting of the transdermal capacity profile, are given in the lower right-hand corner of each plot; other fitted parameters are given in Table 2, and methods are described in the Appendix. $r^2 > 0.99$ in all cases.

Table 2. Parameter values for the model (Eqn 11) fitted to light responses of *E. maculata* and *E. pauciflora* (data of Evans *et al*. (1993), as shown in Fig. 7. Coefficients of determination ranged from 0.991 to 0.999

			E. maculata		*E. pauciflora*	
Parameter	Symbol	Units	Horizontal	Vertical	Horizontal	Vertical
Electron transport capacity	J_m	μmol e^- m^{-2} s^{-1}	139	123	184	182
Max. quantum yield of electrons	ϕ	e^-/photon	0.162	0.145	0.162	0.165
Adaptive weighting for upper surface	w_u	unitless	0.676	0.554	0.680	0.512
Transmittance to non-reflected light	τ	unitless	0.038	0.062	0.077	0.025
Convexity parameter relevant to Eqn 11	Θ_s	unitless	0.836	0.864	0.824	0.906
Modal irradiance (I at which $J_i = J_m$)	$I*$	μE m^{-2} s^{-1}	854	852	1140	1102

mination at either surface should be plastic, at least for some time during leaf development. For example, if a leaf is grown horizontally for a while and then inverted so that its abaxial surface faces upwards, it should eventually respond more favourably to abaxial illumination. This behaviour has in fact been reported numerous times (Terashima 1986; Leverenz 1988; Ögren & Evans 1993). The second corollary is that capacity should be higher at either surface than in the center of leaves that receive significant illumination at both surfaces. This was suggested by Evans *et al*. (1993), who used the numerical model of Terashima & Saeki (1985) to interpret their data, allowing the photosynthetic capacity of each paradermal layer to vary independently to produce a best fit to the observed whole-leaf responses. The fitted transdermal capacity profiles were highest at the upper surface for horizontally restrained leaves and roughly symmetrical for vertically restrained leaves, but lowest in the centre of the leaf in all cases. Consistent with this, Sun, Nishio & Vogelmann (1996) found that extremely high light (4000 μE m^{-2} s^{-1} for 4 h) caused the greatest damage to medial tissues, suggesting adaxial and abaxial tissues were physiologically adapted to higher space irradiances than medial tissues. More direct evidence was recently found by Evans & Vogelmann (2003), who inferred the capacity profile from fluorescence and found the requisite medial 'dip.' Nishio, Sun & Vogelmann (1993) also found a slight rise in Rubisco capacity per unit of chlorophyll near the lower surface of a sun leaf, but not a shade leaf, of spinach.

Any difference in stomatal conductance between the two leaf surfaces may influence the extent to which CO_2 diffusion can adapt to changes in the transdermal distribution of photosynthetic CO_2 demand, and hence may also affect the response of photosynthesis to leaf inversion (e.g. Olsson & Leverenz 1994). In the limiting case of a hypo- or epistomatous leaf, $[CO_2]$ declines within the leaf with increasing distance from the stomatal surface. Thus, when the non-stomatal surface is lit, layers with more light will have less CO_2.

Our model versus the standard model

There are two essential differences between our model and the standard model for J. One is the fixed, non-uniform transdermal profile of electron transport capacity (j_m), in our model, which is what causes different responses to light supplied at the upper and lower surfaces. The second difference is the order in which the mathematical operations of integration and hyperbolic minimization are applied to the profiles of j_m and j_i. The standard model integrates first (thus reducing the capacity and light profiles from transdermally explicit functions to scalar quantities), then hyperbolically minimizes: $\min\{J_i, J_m, \Theta_J\} = \min\{\int j_i dc, \int j_m dc\}$. The better approach would be first to minimize hyperbolically, then to integrate; that is, apply *minh* inside the integral, rather than outside ($\int \min\{j_i, j_m, \theta_j\}$), however, the resulting integral can not be expressed in reduced form. We got around this problem by minimizing non-hyperbolically before integrating, and then accounting for co-limitation by applying *minh* to the integrals of the minimum and maximum profiles. Thus, our model minimizes, integrates, and accounts for co-limitation, in that order: $\min\{J_i - J_s,\ J_m + J_s,\ \Theta_s\} = \min\{\int\min\{j_i, j_m\}, \int\max\{j_i, j_m\}, \Theta_s\}$.

The differences among these three approaches explain why the various 'convexity' terms, Θ_J, Θ_s, and θ_j, are not mathematically equivalent to one another: each measures co-limitation between a different pair of quantities (J_i and J_m, $J_i - J_s$ and $J_m + J_s$, and j_i and j_m, respectively). In the standard model, Θ_J must capture not only decoupling between light absorption and electron transport capacity within each layer, but also decoupling between the transdermal gradients of light and capacity. In our model, the term J_s captures most of the effect of the measurement lighting regime, thus allowing Θ_s to be treated as a constant for a given leaf. However, because our model applies convexity after integrating over the leaf, it imprints Θ_s with the information about the shape of the capacity profile (encoded in w_u and τ), with the result that Θ_s must vary among leaves to account for variation in those properties. The layer-scale convexity parameter (θ_j) needs only to capture decoupling within each layer, so it has no direct dependence on either lighting regime or the leaf's optical geometry.

The relationship between Θ_J and Θ_s has a convenient and useful mathematical formulation. In particular, the standard model matches our model at $I = I*$ when the former uses a special value of Θ_J given by:

$$\Theta_J^*(W_u, w_u) = 1 - [1 - (1 + \sqrt{1 - z\Theta_s})/z]^2, \quad \text{where}$$
$$z \equiv 1 - \left[\left(\frac{1-\sqrt{\tau}}{1+\sqrt{\tau}}\right)(W_u - w_u)\right]^2 \qquad (12)$$

This expression (plotted in Fig. 8, and derived as Eqns 42 and 44 in the Appendix) shows how the apparent convexity of light-response curves depends on both the lighting regime (W_u) and the leaf's optical geometry (w_u and τ). Equation 12 provides a tool for interpreting the variation in Θ_J reported for upper and lower leaf surfaces, and for expressing in succinct form the model's predictions about the effects of leaf inversion on convexity. We compared the predictions of Eqn 12 with values of Θ_J fitted to light-response curves by Evans *et al.* (1993) under various growth and measurement lighting regimes, and found reasonable qualitative agreement (Fig. 8).

Other models

Several other transdermally explicit models for photosynthesis or potential electron transport rate exist in the literature. We are aware of two analytical models (Badeck 1995; Kull & Kruijt 1998), both of which assume that electron transport capacity is uniform among paradermal chlorophyll layers (i.e. j_m is a constant over c). This precludes the ability to predict different responses to illumination at either surface, and it contrasts with most experiments, which have found that the transdermal profiles of light absorption, carbon fixation, Rubisco activity, photosynthetic activity, and photo-inhibitory sensitivity are strongly non-uniform (Terashima & Inoue 1984, 1985a; b; Nishio *et al.* 1993; Sun *et al.* 1996; Evans & Vogelmann 2003). Our model prescribes an explicitly non-uniform capacity profile, so it is a step towards accommodating those results.

Other transdermally explicit models permit non-uniform transdermal capacity profiles but require numerical integration over paradermal layers. Terashima & Saeki (1985) presented a numerical model with 10 paradermal layers, of which the upper four layers (representing the 'palisade' mesophyll) had one value for photosynthetic capacity, while the lower six ('spongy') layers had a different capacity, and all layers had distinct optical properties measured by experiment. That model predicted that light-use efficiency should increase with the ratio of palisade to spongy photosynthetic capacity when the upper surface is illuminated. Ustin, Jacquemoud & Govaerts (2001) reached a similar conclusion, using a highly sophisticated three-dimensional numerical model of transdermal light propagation coupled to a simple photosynthesis model.

Ustin *et al.* (2001) also concluded that the profiles of carbon fixation and light were decoupled, as earlier reported by Nishio *et al.* (1993). However, the decoupling in their simulations was a consequence of the bimodal capacity profile that they assumed; if, instead, they had assumed a capacity profile that matched their predicted light absorption profiles, the decoupling would necessarily have disappeared. Evans (1995) showed that the apparent decoupling observed by Nishio *et al.* (1993) was in fact caused by incongruence of the spatial profiles of space irradiance and light absorption, which resulted, in turn, from spatial inhomogeneity in absorption characteristics. When the data were re-ordinated to the light-absorbing axis of

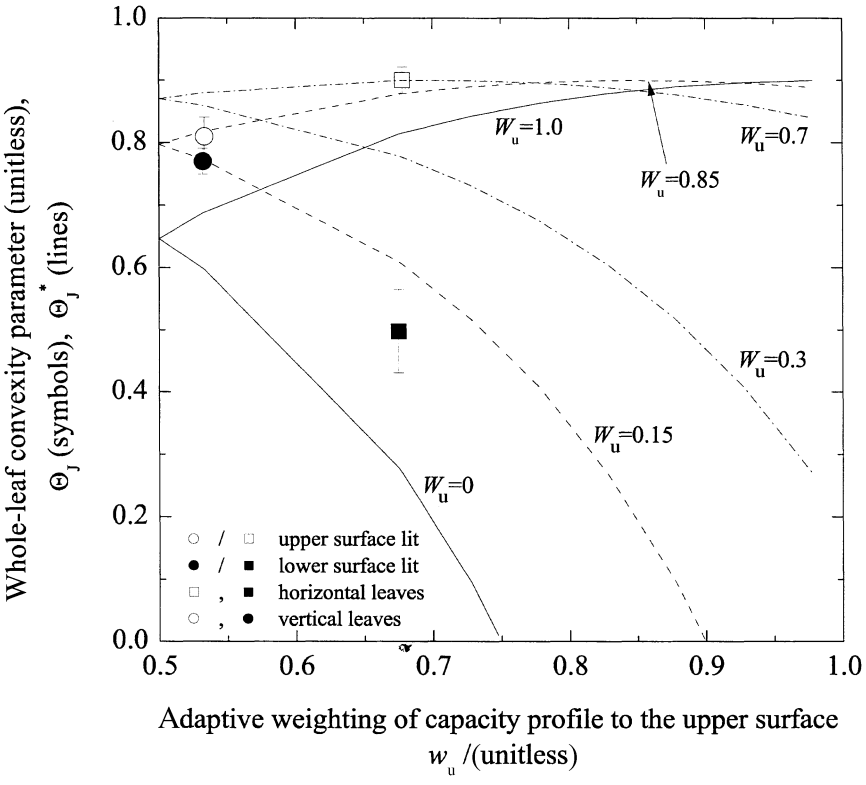

Figure 8. Lines: Value of the whole-leaf convexity parameter that causes the standard model (Eqn 1) to match our model (Eqn 11) at $I = I*$, as calculated from Eqn 12, for six values of W_u (as labelled), and $\tau = 0.051$ (the average fitted value from Fig. 7) and $\Theta_s = 0.90$ (the greatest of the measured values indicated by symbols). Symbols: Mean values of Θ_J measured by Evans *et al.* (1993) for horizontally grown (□, ■) or vertically grown leaves (○, ●) illuminated at the upper (□, ○) or lower surfaces (■, ●). Vertical error bars are measured SEs for three to eight leaves of four species. Horizontal leaves were assumed to have the same average w_u values as the horizontal leaves to which Eqn 11 was fitted in Fig. 7 ($w_u = 0.678$), and likewise for vertical leaves ($w_u = 0.533$).

cumulative chlorophyll content, and the fixation profile was compared with the profile of absorption, rather than that of space irradiance, the two profiles matched very well (as later confirmed experimentally by Evans & Vogelmann 2003). Our model codifies those insights by ordinating the transdermal axis by cumulative chlorophyll content rather than by spatial position. Therefore, while the 'layers' in our model may represent paradermal layers of different thickness or cell type (e.g. palisade versus spongy), each layer has equal absorptance by definition. Because of this abstraction, to make our model directly commensurate with spatially ordinated measurements (e.g. Nishio *et al*. 1993) or models (e.g. Ustin *et al*. 2001), the spatial distribution of chlorophyll must be known.

SUMMARY

A new analytical model is presented for whole-leaf potential electron transport rate (J). The model predicts different responses to illumination at either leaf surface, it can accommodate varying degrees of preference for lighting at each leaf surface, and it is consistent with observed transdermal profiles of photosynthetic capacity, and with observed effects of leaf inversion, during both growth and measurement, on whole-leaf light responses. Our model captures these features with a fairly small mathematical cost of two additional parameters (the adaptive weighting of the capacity profile, w_u, and the transmittance to non-reflected light, τ) and one independent variable (the irradiance at the upper or lower surface, I_u or I_l), and its parameters are readily estimated from light-response curves. We suggest the model as a replacement for the more commonly used expression (Eqn 1) in cases where one wishes to account for variation in the proportions of irradiance arriving at either leaf surface, and/or variation in the adaptive preferences of leaves for illumination of either leaf surface.

ACKNOWLEDGMENTS

T.N.B. thanks John Evans for many suggestions and insights that led to the present development and for providing the data in Figs 7 and 8, and Belinda Barnes for verifying the futility of attempting to integrate Eqn 19.

REFERENCES

Badeck F.-W. (1995) Intra-leaf gradient of assimilation rate and optimal allocation of canopy nitrogen: a model on the implications of the use of homogeneous assimilation functions. *Australian Journal of Plant Physiology* **22,** 425–439.

DeLucia E.H., Shenoi H.D., Naidu S.L. & Day T.A. (1991) Photosynthetic symmetry of sun and shade leaves of different orientations. *Oecologia* **87,** 51–57.

Evans J.R. (1995) Carbon fixation profiles do reflect light absorption profiles in leaves. *Australian Journal of Plant Physiology* **22,** 865–873.

Evans J.R. & Vogelmann T.C. (2003) Profiles of ^{14}C fixation through spinach leaves in relation to light absorption and photosynthetic capacity. *Plant, Cell and Environment* **26,** 547–560.

Evans J.R., Jakobsen I. & Ögren E. (1993) Photosynthetic light-response curves. 2. Gradients of light absorption and photosynthetic capacity. *Planta* **189,** 191–200.

Farquhar G.D. (1989) Models of integrated photosynthesis of cells and leaves. *Philosophical Transactions of the Royal Society of London, Series B* **323,** 357–367.

Farquhar G.D. & Wong S.C. (1984) An empirical model of stomatal conductance. *Australian Journal of Plant Physiology* **11,** 191–210.

Farquhar G.D., von Caemmerer S. & Berry J.A. (1980) A biochemical model of photosynthetic CO_2 assimilation in leaves of C_3 species. *Planta* **149,** 78–90.

Kirschbaum M.U.F. (1984) *The Effects of Light, Temperature, and Water Stress on Photosynthesis in Eucalyptus pauciflora, Thesis* Australian National University, Canberra, Australia.

Kubelka V.P. & Munk F. (1931) Ein beitrag zur optic der farbanstriche. *Zeitschrift Fur Technische Physik* **11,** 593–601.

Kull O. & Kruijt B. (1998) Leaf photosynthetic light response: a mechanistic model for scaling photosynthesis to leaves and canopies. *Functional Ecology* **12,** 767–777.

Leverenz J.W. (1988) The effects of illumination sequence, CO_2 concentration, temperature and acclimation on the convexity of the photosynthetic light response curve. *Physiologia Plantarum* **74,** 332–341.

Moss D.N. (1964) Optimum lighting of leaves. *Crop Science* **4,** 131–136.

Nishio J.N., Sun J. & Vogelmann T.C. (1993) Carbon fixation gradients across spinach leaves do not follow internal light gradients. *Plant Cell* **5,** 953–961.

Ögren E. & Evans J.R. (1993) Photosynthetic light response curves. I. The influence of CO_2 partial pressure and leaf inversion. *Planta* **189,** 182–190.

Olsson T. & Leverenz J.W. (1994) Non-uniform stomatal closure and the apparent convexity of the photosynthetic photon flux density response curve. *Plant, Cell and Environment* **17,** 701–710.

Sun J., Nishio J.N. & Vogelmann T.C. (1996) High-light effects on CO_2 fixation gradients across leaves. *Plant, Cell and Environment* **19,** 1261–1271.

Terashima I. (1986) Dorsiventrality in photosynthetic light response curves of a leaf. *Journal of Experimental Botany* **37,** 399–405.

Terashima I. & Inoue Y. (1984) Comparative photosynthetic properties of palisade tissue chloroplasts and spongy tissue chloroplasts of *Camellia japonica* L. functional adjustment of photosynthetic apparatus to light environment within a leaf. *Plant and Cell Physiology* **25,** 555–563.

Terashima I. & Inoue Y. (1985a) Palisade tissue chloroplasts and spongy tissue chloroplasts in spinach: biochemical and ultrastructural differences. *Plant and Cell Physiology* **26,** 63–75.

Terashima I. & Inoue Y. (1985b) Vertical gradients in photosynthetic properties of spinach chloroplasts dependent on intraleaf light environment. *Plant and Cell Physiology* **26,** 781–785.

Terashima I. & Saeki T. (1985) A new model for leaf photosynthesis incorporating the gradients of light environment and of photosynthetic properties of chloroplasts within a leaf. *Annals of Botany* **56,** 489–499.

Ustin S.L., Jacquemoud S. & Govaerts Y. (2001) Simulation of photon transport in a three-dimensional leaf: implications for photosynthesis. *Plant, Cell and Environment* **24,** 1095–1103.

Vogelmann T.C. & Bjorn L.O. (1984) Measurement of light gradient and spectral regime in plant tissue with a fibre optic probe. *Physiologia Plantarum* **60,** 361–368.

Received 29 March 2004; received in revised form 11 June 2004; accepted for publication 14 June 2004

APPENDIX

We divide the leaf into infinitesimal paradermal layers, each having the same amount of chlorophyll per unit of leaf area, dc. This defines an axis of cumulative chlorophyll content, c, ranging from 0 at the upper surface to C, the whole-leaf chlorophyll content, at the 'lower' surface (units for all terms are given in Table 1). The upper surface is arbitrarily defined as the one whose normal vector points above the horizon (regardless of its ontogenetic status as adaxial or abaxial), and we denote the upper and lower surfaces with subscripts 'u' and 'l', respectively.

Transdermal light propagation and capture

Kubelka & Munk (1931) developed equations to describe light propagation within leaves. Their theory accounts for reflection among paradermal chlorophyll layers, which can increase the total flux of photons passing through each layer (the 'space irradiance'; Vogelmann & Bjorn 1984), and can cause some light that has entered the leaf to be reflected back out of the same surface. Kirschbaum (1984) extended the Kubelka–Munk theory to account for the angular dependence of absorptance and reflectance among paradermal layers, and found that the predicted profiles of space irradiance and light absorption can be described adequately by exponential functions. However, the space irradiance in layers near the illuminated surface is predicted to be higher than the incident irradiance, due to internal reflection, so the space irradiance profile is larger than the simple exponential predicted by Beer's Law by a factor $p' > 1$:

$$i_u(I_u, c) = p' I_u e^{-k_c c}. \quad (13)$$

where $i_u(c)$ is space irradiance due to illumination of the upper surface, I_u is incident irradiance at the upper surface, and k_c is the sum of absorption and scattering coefficients. Kirschbaum's simulations also suggested that the angle of incidence of incoming radiation strongly affects the fraction of light reflected from the upper leaf surface (the surface reflectance, ρ), but that, of light not reflected at the surface, the fraction that is transmitted (τ) varied little with angle of incidence. Hence, we may resolve p' to $p(1-\rho)$, where p accounts strictly for internal reflection and may be considered independent of the angle of incidence, whereas ρ, the surface reflectance, depends on the angle of incidence. If the angular distribution of photons moving within the leaf does not vary among paradermal chlorophyll layers, then the absorptance of each layer will also be conserved among layers, in which case the rate of absorption of photons that entered the upper leaf surface, $i_{au}(c)$, is simply proportional to the space irradiance by an absorption coefficient, k_c':

$$i_{au}(I_u, c) = p(1-\rho) k_c' I_u e^{-k_c c} \quad (14)$$

The absorption coefficient, k_c', differs from the apparent extinction coefficient for the space irradiance profile, k_c, because the latter is the sum of absorption and scattering coefficients (Kirschbaum 1984). Most leaves will also receive some light at their lower surface for at least some part of a typical day, and the profile of light absorption for photons coming from that surface can be modelled in the same fashion as for the upper surface, except that the direction of propagation is reversed, making the exponential operand $-k_c(C-c)$ rather than $-k_c c$:

$$i_{al}(I_l, c) = p(1-\rho) k_c' I_l e^{-k_c(C-c)} = p(1-\rho) k_c' \tau I_l e^{+k_c c} \quad (15)$$

where I_l is the incident irradiance at the lower surface and is the transmittance of the leaf to non-reflected (as distinct from incident) light. Note that this 'τ' differs from the conventional transmittance; the latter is defined as the complement of absorptance and reflectance ($1-\alpha-\rho$), whereas τ here is related to absorptance by the relation $\alpha = (1-\tau)(1-\rho)$, or equivalently, $\tau = (1-\alpha-\rho)/(1-\rho)$ (Fig. 9). The main reason for choosing this convention was mathematical expediency – it makes the resulting model formulation simpler.

The total rate of photon capture by layer c is the sum of Eqns 14 and 15:

$$i_a(I_u, I_l, c) = p(1-\rho) k_c' (I_u e^{-k_c c} + \tau I_l e^{k_c c}). \quad (16)$$

Components of potential electron transport rate in each paradermal layer

We assume that the potential electron transport rate of a single paradermal chlorophyll layer, $j(c)$, can be accurately modelled as a hyperbolic minimum of two limiting rates: a light-limited rate ($j_i(c)$) and a rate limited by local electron transport capacity ($j_m(c)$). To calculate the light-limited rate, we assume that a fraction f' of the absorbed photons do not contribute to photochemistry, and that the others free electrons from water with an efficiency ϕ_m; hence $j_i(c)$ may be written

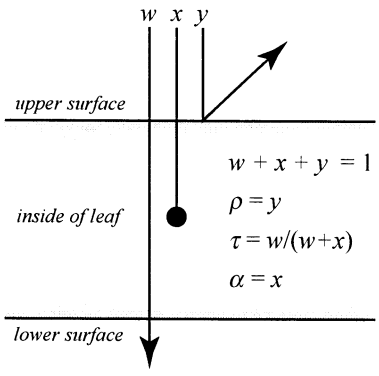

Figure 9. Diagram explaining the relationship among surface reflectivity (ρ), absorptance (α) and transmittance to non-reflected light (τ). The three lines (w,x,y) represent complementary fractions of the total photon flux incident on the leaf surface; w is transmitted, x is absorbed, and y is reflected. The quantity 'τ' in our model is not w, but rather, the ratio $w/(w+x)$, or equivalently, $w/(1-y)$. However, the surface reflectance ρ and leaf absorptance α are simply equal to y and x, respectively.

$$j_i(I_u, I_l, c) = \phi_m(1-f')i_a(I_u, I_l, c) = k_c F\left(I_u e^{-k_c c} + \tau I_l e^{k_c c}\right), \quad (17)$$

where $F^\circ \equiv \phi_m(1-f')p(1-\rho)k_c'/k_c$. We further hypothesize that the transdermal profile of electron transport capacity, $j_m(c)$, is a weighted average of two j_i profiles, each of which corresponds to illumination of only one surface at some 'preferred' irradiance, $I*$:

$$j_m(c) = w_u j_i\left(I_*, 0, c\right) + w_l j_i\left(0, I_*, c\right) = k_c F I_*\left(w_u e^{-k_c c} + \tau w_l e^{k_c c}\right). \quad (18)$$

The 'adaptive weightings' towards the upper and lower surfaces, w_u and w_l, respectively, sum to unity ($w_u + w_l \equiv 1$) by definition. The potential electron transport rate for a single layer is then given by

$$\begin{aligned} j(c) &= \min\{j_i(c), j_m(c), \theta_j\} \\ &= (1/2\theta_j)\left(j_i + j_m - \sqrt{j_i^2 + j_m^2 + (2-4\theta_j)j_i j_m}\right). \end{aligned} \quad (19)$$

Integrating to the leaf

Whole-leaf potential electron transport rate, J, is the integral of Eqn 19 over c:

$$\begin{aligned} J &= \int_0^C j(c)\mathrm{d}c \\ &= (1/2\theta_j)\left(\int_0^C j_i \mathrm{d}c + \int_0^C j_m \mathrm{d}c - \int_0^C \sqrt{j_i^2 + j_m^2 + (2-4\theta_j) j_i j_m}\mathrm{d}c\right) \end{aligned} \quad (20)$$

The first two integrals in Eqn 20 are easily computed. The first is simply the whole-leaf light-limited rate, mathematically identical to the term J_i in the standard model (Eqn 1):

$$\begin{aligned} \int_0^C j_i(c)\mathrm{d}c &= \int_0^C k_c F(I_u e^{-k_c c} + \tau I_l e^{k_c c})\mathrm{d}c \\ &= FI_*[-\omega_u e^{-k_c c} + \tau\omega_l e^{k_c c}]_0^C \\ &= FI_*[\omega_u(1-e^{-k_c c}) + \tau\omega_l(e^{k_c c}-1)] \\ &= (1-\tau)F(I_u + I_l) = \phi(I_u + I_l) = \phi I \equiv J_i \end{aligned} \quad (21)$$

(where ω_u and ω_l are shorthand for the ratios $I_u/I*$ and $I_l/I*$), and the second integral in Eqn 20 is identical to the maximum potential electron transport rate, J_m, in the standard model:

$$\begin{aligned} \int_0^C j_m(c)\mathrm{d}c &= \int_0^C k_c F I_*(w_u e^{-k_c c} + \tau w_l e^{k_c c})\mathrm{d}c \\ &= FI_*[-w_u e^{-k_c c} + \tau w_l e^{k_c c}]_0^C \\ &= FI_*[w_u(1-e^{-k_c c}) + \tau w_l(e^{k_c c}-1)] \\ &= (1-\tau)FI_*(w_u + w_l) = \phi I_* \equiv J_m \end{aligned} \quad (22)$$

The third integral on the right-hand side of Eqn 20, however, can not be computed analytically. Applying Eqns 17 and 18 and making the substitution transforms the integral to

$$-\frac{1}{2}FI_*\int_{\tau^2}^1 v^{-3/2}\sqrt{a_2 v^2 + a_1 v + a_0}\,\mathrm{d}v, \quad (23)$$

(where the a_k are real and non-negative: $a_2 = \omega_u^2 + w_u^2$, $a_1 = 2\tau(\omega_u\omega_l + w_u w_l)$, and $a_0 = \tau^2(\omega_l^2 + w_l^2)$), which is an elliptic integral with no general closed-form solution (Belinda Barnes, personal communication).

We will proceed to develop an approximate solution for J by integrating the simple minimum of $j_i(c)$ and $j_m(c)$; subsequently, we will attempt to account for the effect of convexity in the response of j to j_i and j_m within individual chlorophyll layers. The integral of the simple minimum requires four separate cases to be considered (illustrated in Fig. 4). Cases 1 and 2 apply when the profiles of j_i and j_m do not cross over within the leaf (e.g. Fig. 4a & b). Cases 3 and 4 come into play when there is a cross-over point; case 3 applies when the upper surface is light-saturated (Fig. 4c), and case 4 applies when the lower surface is light-saturated (Fig. 4d).

The first step is to generate a test to determine whether the profiles cross over within the leaf. Cross-over points are found by equating j_i with j_m and solving for c:

$$c^*(I_u, I_l) = \frac{C}{2} + \frac{1}{2k_c}\ln s_u \left(= \frac{C}{2} - \frac{1}{2k_c}\ln s_l\right), \text{ where} \quad (24)$$

$$s_u \equiv -\frac{\omega_u - w_u}{\omega_l - w_l} = -\frac{I_u - w_u I_*}{I_l - w_l I_*} = -\frac{\phi I_u - w_u J_m}{\phi I_l - w_l J_m} \quad \text{and} \quad s_l \equiv \frac{1}{s_u}. \quad (25)$$

If $0 < c^* < C$, a cross-over point $c = c^*$ lies within the leaf. This condition can be expressed in terms of whole-leaf variables by setting c^* equal to 0 and C:

$$\begin{aligned} 0 &= C/2 + \ln s_u/2k_c \rightarrow -k_c C = \ln s_u \rightarrow \tau = s_u \\ C &= C/2 + \ln s_u/2k_c \rightarrow +k_2 C = \ln s_u \rightarrow \tau^{-1} = s_u \end{aligned} \quad (26)$$

Thus, the profiles cross within the leaf if s_u is between τ and $1/\tau$. If this condition is not satisfied, then either $j_i > j_m$ in all layers, or $j_m > j_i$ in all layers, so $\int\min\{j_i, j_m\}\mathrm{d}c = \min\{\int j_i\mathrm{d}c, \int j_m\mathrm{d}c\}$, that is

$$\int_0^C \min\{j_i(c), j_m(c)\}\mathrm{d}c = \min\{J_i, J_m\} \quad if \quad s_u \notin (\tau, \tau^{-1}) \quad (27)$$

Equation 27 covers cases 1 and 2 for the integral. If instead s_u is between τ and τ^{-1}, then we must decide between the third and fourth cases; this requires a test to determine which surface (upper or lower) is light-saturated. The upper surface is saturated if $j_i(0) > j_m(0)$, which, from Eqns 17 and 18, implies $I_u + \tau I_l > w_u I_* + \tau\ w_l I_*$, or equivalently, $w_u - \omega_u < -\tau(w_l - \omega_l)$. However, this may be simplified to $w_u - \omega_u < 0$ by the requirement that $s_u > \tau$. (To prove this, we will show that $w_u - \omega_u < 0$ and $s_u > \tau$ together imply $w_u - \omega_u < -\tau(w_l - \omega_l)$. First, $s_u > \tau$ implies $-(w_u - \omega_u)/(w_l - \omega_l) > \tau$, which in turn implies either $-(w_u - \omega_u) > \tau(w_l - \omega_l)$ (if $w_l - \omega_l > 0$), or $-(w_u - \omega_u) < -\tau(w_l - \omega_l)$ (if $w_l - \omega_l < 0$). However, $s_u > \tau$ also requires that $s_u > 0$, which is possible only if $w_u - \omega_u$ and $w_l - \omega_l$ have different signs; as we assumed $w_u - \omega_u < 0$, $w_l - \omega_l$ must be positive, and hence $-(w_u - \omega_u) > \tau(w_l - \omega_l)$, or equivalently $w_u - \omega_u < -\tau(w_l - \omega_l)$, which is what we set out to prove.) Therefore, $w_u - \omega_u < 0$ (equivalently, $I_u > w_u I*$) is a sufficient condition to ensure $j_i(0) > j_m(0)$ when the profiles cross over within the leaf. If this condition is satisfied, then the third case for the integral applies, and we must integrate the upper and lower parts of the leaf separately. Between the upper surface and the

cross-over point ($c < c^*$), $\min\{j_i,j_m\} = j_m$; below the cross-over point, $\min\{j_i,j_m\} = j_i$. Thus, we integrate j_m from $c = 0$ to c^*, and j_i from c^* to C:

$$\int_0^C \min\{j_i, j_m\}\mathrm{d}c = \int_0^{c^*} j_m(c)\mathrm{d}c + \int_{c^*}^C j_i(c)\mathrm{d}c \quad \text{if} \quad s_u \in (\tau, \tau^{-1}) \quad \text{and} \quad I_u > w_u I_* \tag{28}$$

The condition for the fourth case is the opposite of that for the third case, namely $I_u < w_u I_*$. When this condition is satisfied, we integrate j_i from 0 to c^*, and j_m from c^* to C:

$$\int_0^C \min\{j_i, j_m\}\mathrm{d}c = \int_0^{c^*} j_i(c)\mathrm{d}c + \int_{c^*}^C j_m(c)\mathrm{d}c \quad \text{if} \quad s_u \in (\tau, \tau^{-1}) \quad \text{and} \quad I_u < w_u I_* \tag{29}$$

Now we evaluate these piecewise integrals. For the third case (Eqn 28), the first integral is

$$\begin{aligned}\int_0^{c^*} j_m(c)\mathrm{d}c &= FI_*[-w_u e^{-k_c c} + \tau w_u e^{k_c c}]_0^{c^*} \\ &= FI_*[-w_u(e^{-k_c c^*} - 1) + \tau w_l(e^{k_c c^*} - 1)] \\ &= FI_*[w_u(1 - \sqrt{\tau/s_u}) + \tau w_l(\sqrt{s_u/\tau} - 1)]\end{aligned} \tag{30}$$

and the second integral is

$$\begin{aligned}\int_{c^*}^C j_i(c)\mathrm{d}c &= FI_*[-w_u e^{-k_c c} + \tau w_l e^{k_c c}]_{c^*}^C \\ &= FI_*[-\omega_u(\tau - e^{-k_c c^*}) + \tau\omega_l(\tau^{-1} - e^{k_c c^*})] \\ &= FI_*[\omega_u(\sqrt{\tau/s_u} - \tau) + \tau\omega_l(\tau^{-1} - \sqrt{s_u/\tau})]\end{aligned} \tag{31}$$

To complete the integral in Eqn 28, we add Eqns 30 and 31 to give

$$\begin{aligned}&= FI_*[\tau(w_l - \omega_l)\sqrt{s_u/\tau} + (\omega_u - w_u)\sqrt{\tau/s_u} + \omega_l + w_u \\ &\quad - \tau(\omega_u + w_l)] \\ &= FI_*[2\sqrt{\tau(\omega_u - w_u)(w_l - \omega_l)} + \omega_l + w_u \\ &\quad - \tau(\omega_u + w_l)]\end{aligned} \tag{32}$$

The second step in Eqn 32 results by applying Eqn 25 and pulling $\tau(w_l - \omega_l)$ and $(\omega_u - w_u)$ into the radicals. We note now that the remaining radical is the central term when the binomial $\sqrt{w_l - \omega_l} - \sqrt{\tau(\omega_u - w_u)}$ is squared. We may complete that square to give

$$\begin{aligned}&= FI_*\Big[(w_l - \omega_l) + \tau(\omega_u - w_u) - \left(\sqrt{w_l - \omega_l} - \sqrt{\tau(\omega_u - w_u)}\right)^2 \\ &\quad + \omega_l + w_u - \tau(\omega_u + w_l)]\end{aligned} \tag{33}$$

and cancel terms to give

$$\begin{aligned}&= FI_*\Big[-\left(\sqrt{w_l - \omega_l} - \sqrt{\tau(\omega_u - w_u)}\right)^2 + (1 - \tau)(w_u + w_l)\Big] \\ &= (1 - \tau)F(I_u + I_l) - (1 - \sqrt{\tau s_u})^2 F\big(I_l - w_l I_*\big)\end{aligned} \tag{34}$$

The first term in Eqn 34 is simply J_i (cf. Eqn 21), and we may define the second term by the new symbol $J_{s,l}$. Thus, when the profiles cross within the leaf and the upper surface is light-saturated (case 3), the integral of $\min\{j_i,j_m\}$(Eqn 28) is $J_i - J_{s,l}$.

The piecewise integrals for case 4 (Eqn 29) are readily evaluated by comparison with Eqns 30 and 31, with ω replacing w and vice versa:

$$\int_0^{c^*} j_i(c)\mathrm{d}c = FI_*[\omega_u(1 - \sqrt{\tau/s_u}) + \tau\omega_l(\sqrt{s_u/\tau} - 1)], \text{and} \tag{35}$$

$$\int_{c^*}^C j_m(c)\mathrm{d}c = FI_*[\omega_u(\sqrt{\tau/s_u} - \tau) + \tau\omega_l(\tau^{-1} - \sqrt{s_u/\tau})] \tag{36}$$

We add these to give

$$\begin{aligned}&= FI_*[\omega_u(1 - \sqrt{\tau/s_u}) + \tau\omega_l(\sqrt{s_u/\tau} - 1) + w_u(\sqrt{\tau/s_u} - \tau) \\ &\quad + \tau w_l(\tau^{-1} - \sqrt{s_u/\tau})] \\ &= FI_*[\tau(\omega_l - \omega_l)\sqrt{s_u/\tau} + (w_u - \omega_u)\sqrt{\tau/s_u} + \omega_u + w_l \\ &\quad - \tau(w_u + \omega_l)] \\ &= FI_*[2\sqrt{\tau(\omega_l - w_l)(w_u - \omega_u)} + \omega_u + w_l - \tau(w_u + \omega_l)]\end{aligned} \tag{37}$$

Once again completing the square and rearranging as in Eqns 33 and 34, we have

$$\begin{aligned}&= FI_*[(\omega_l - w_l) + \tau(w_u - \omega_u) \\ &\quad - \left(\sqrt{w_u - \omega_u} - \sqrt{\tau(\omega_l - w_l)}\right)^2 + \omega_u + w_l - \tau(w_u + \omega_l)\Big] \\ &= (1 - \tau)F(I_u + I_l) - (1 - \sqrt{\tau/s_u})^2 F\big(I_u - w_u I_*\big)\end{aligned} \tag{38}$$

Once again, the first term is J_i, we define the second as $J_{s,u}$, and Eqn 29 integrates to $J_i - J_{s,u}$. Because the terms $J_{s,l}$ and $J_{s,u}$ (Eqns 34 and 38) are algebraically similar, they may be combined using the notation

$$J_s = (\phi I_{u(l)} - w_{u(l)} J_m)\left(\frac{1 - \sqrt{\tau/s_{u(l)}}}{\sqrt{1 - \tau}}\right)^2 \quad \text{if} \quad s_u \in (\tau, \tau^{-1}) (\text{else } J_s = 0) \tag{39}$$

where 'u(l)' refers to the light-saturated surface (the upper surface if $I_u > w_u I_*$, or the lower surface if $I_l > w_l I_*$). (Note that to generalize and simplify the notation, we have replaced s_u in Eqn 34 with $1/s_l$, as defined in Eqn 25, replaced F with $\phi/(1 - \tau)$, and replaced I_* with J_m/ϕ.) This is Eqn 9 in the main text, where it is expressed without the conditional notation.

To summarize the four cases for the integral of $\min\{j_i,j_m\}$: When s_u is not between τ and $1/\tau$, the integral is simply $\min\{J_i,J_m\}$ (this covers cases 1 and 2). When s_u is between τ and $1/\tau$, the integral is $\min\{J_i - J_s,J_m\}$; this covers cases 3 and 4, which are distinguished using the conditional notation u(l) in Eqn 38. Furthermore, because $J_s = 0$ in cases 1 and 2 by definition, $\min\{J_i - J_s,J_m\}$ covers those cases as well. Therefore, we may write a single expression for all four cases:

$$\int_0^C \min\{j_i(c), j_m(c)\}\mathrm{d}c = \min\{J_i - J_s, J_m\} \tag{40}$$

Accounting for convexity

Equation 40 is equal to the integral of Eqn 20 only if $\theta_j = 1$. Although Eqn 20 can not be integrated analytically for $\theta_j < 1$, the effects of layer-scale convexity may be accounted for, in part, by calculating the hyperbolic minimum of $J_i - J_s$ and $J_m + J_s$, which are the integrals of the layerwise minima and the layerwise maxima of j_i and j_m (as illustrated in Fig. 3f & e), namely $\int\min\{j_i,j_m\}\mathrm{d}c$ and $\int\max\{j_i,j_m\}\mathrm{d}c$:

$$J = \mathrm{minh}\{J_i - J_s, J_m + J_s, \Theta_s\} \tag{41}$$

Note that, when the whole leaf is light-saturated, $J_s = 0$ and $J_i > J_m$, in which case $J_i - J_s$ is the integral of the layerwise *maxima*, and $J_m + J_s$ is the integral of the minima.

Relationship between Θ_J and Θ_s

The shape of the whole-leaf light-response curve is affected by the lighting regime both during measurement and during growth. In the standard model, the curvature parameter Θ_J must vary to capture both of these effects, whereas in our model, the convexity parameter Θ_s is independent of measurement lighting regime. It is possible, however, to predict how Θ_J would need to vary to mimic the qualitative dependence of the light responses predicted by our model on growth and measurement lighting regimes.

We make use of a convenient feature of the hyperbolic minimum function: when $J_i = J_m$ in the standard model, $J = J_m(1-\sqrt{1-\Theta_J})/\Theta_J$ (which is readily verified by substituting J_i for J_m in Eqn 1). This can be simplified by writing Θ_J as $(1-(1-\Theta_J))$, factoring to give $(1-\sqrt{1-\Theta_J})(1+\sqrt{1-\Theta_J})$, and cancelling terms to yield $J = J_m/(1+\sqrt{1-\Theta_J})$. Similarly, our model (Eqn 41) reduces to $J = J_m\left(1-\sqrt{1-\Theta_s\left(1-J_s^2/J_m^2\right)}\right)/\Theta_s$ when $J_i = J_m$ (to see this, replace J_i with J_m in Eqn 11 and rearrange). Then define $z \equiv 1-J_s^2/J_m^2$, write Θ_s in the denominator as $(z\Theta_s)/z$, and, as for Θ_J above, write $z\Theta_s$ as $1-(1-z\Theta_s)$, factor to $(1-\sqrt{1-z\Theta_s})(1+\sqrt{1-z\Theta_s})$, and cancel terms to give $J = J_m z/(1+\sqrt{1-z\Theta_z})$. Hence the two models coincide when $1+\sqrt{1-\Theta_J} = (1+\sqrt{1-z\Theta_z})/z$, or

$$\Theta_J = 1-(1-(1+\sqrt{1-z\Theta_s})/z)^2 \tag{42}$$

To express z in terms of w_u, τ, and the distribution of light between leaf surfaces, note that, because of the complementarity relations inherent in the identities $I_u + I_l = I$ and $w_u + w_l = 1$, s_u (Eqn 25) can be written as $-\left(I_u - w_u I_*\right)/\left((I-I_u)-(1-w_u)I_*\right) = \left(I_u - w_u I_*\right)/\left(\left(I_u - w_u I_*\right)-\left(I-I_*\right)\right)$.

Then, since $J_i = J_m$ implies $I = I*$, $I - I*$ vanishes in the denominator and $s_u = 1$. By a similar argument, $J_i = J_m$ implies $s_l = 1$, so J_S is simply $(1-\sqrt{\tau})^2 F\left(I_{u(l)} - w_{u(l)} I_*\right)$ from Eqn 39. Now we factor the quantity $(1-\tau)$ in Eqn 22 to write J_m as $(1-\sqrt{\tau})(1+\sqrt{\tau})FI_*$, and compute the ratio of J_s to J_m as

$$\begin{aligned}\frac{J_s}{J_m} &= \frac{\left(1-\sqrt{\tau}^2\right)F\left(I_{u(l)} - w_{u(l)} I_*\right)}{(1-\sqrt{\tau})(1+\sqrt{\tau})FI_*} \\ &= \frac{1-\sqrt{\tau}}{1+\sqrt{\tau}}\left(\frac{I_{u(l)}}{I_*} - w_{u(l)}\right) = \frac{1-\sqrt{\tau}}{1+\sqrt{\tau}}\left(W_{u(l)} - w_{u(l)}\right)\end{aligned} \tag{43}$$

The last step uses $I = I*$ at $J_i = J_m$ and defines the weighting of the lighting regime towards the upper surface (I_u/I) as W_u. Finally, since $(W_u - w_u) = 1 - W_l - (1 - w_l) = -(W_l - w_l)$ and Eqn 42 takes the square of this quantity, the result is the same whether u(l) = u or l, so we can arbitrarily replace u(l) with u and write

$$z = 1-\left(\left(\frac{1-\sqrt{\tau}}{1+\sqrt{\tau}}\right)\left(W_u - w_u\right)\right)^2 \tag{44}$$

Equations 42 and 44 provide a tool for interpreting or predicting the qualitative effects of w_u, W_u, and τ on the apparent convexity of whole-leaf light-response curves.

Model fitting procedure

We fitted our model (Eqns 7–11) to the light-response curves published by Evans *et al*. (1993) as follows. First, we multiplied their measurements of oxygen evolution (gross photosynthesis rate) by 4 to estimate whole-leaf potential electron transport rate (J) (assuming saturating intercellular CO_2 on the grounds that ambient CO_2 was 5.0 kPa). Second, we calculated the initial slope of J versus absorbed irradiance by fitting lines forced through the origin ($n = 7$–8 and $r^2 > 0.97$ in all cases) to measurements at low light ($I < 300\ \mu E\ m^{-2}\ s^{-1}$), averaged the resulting slopes over three light-response curves for each plant treatment (species x growth orientation), and estimated J_i as the product of this slope and absorbed irradiance. Third, we fitted all three complete light responses for each plant treatment to our model (Eqn 11) by least-squares, treating J_i and J as independent and dependent variables, respectively, and allowing J_m, Θ_s, w_u and τ to vary as free parameters.